

Statistics of Kinetic Dissipation in the Earth's Magnetosheath: MMS ObservationsRiddhi Bandyopadhyay ^{*}*Department of Physics and Astronomy, University of Delaware, Newark, Delaware 19716, USA*William H. Matthaeus *Department of Physics and Astronomy, University of Delaware, Newark, Delaware 19716, USA
and Bartol Research Institute, University of Delaware, Newark, Delaware 19716, USA*Tulasi N. Parashar [†]*Department of Physics and Astronomy, University of Delaware, Newark, Delaware 19716, USA*Yan Yang *Southern University of Science and Technology, Shenzhen, Guangdong 518055, China*

Alexandros Chasapis

Laboratory for Atmospheric and Space Physics, University of Colorado Boulder, Boulder, Colorado 80303, USA

Barbara L. Giles and Daniel J. Gershman

NASA Goddard Space Flight Center, Greenbelt, Maryland 20771, USA

Craig J. Pollock

*Denali Scientific, Fairbanks, Alaska 99709, USA*Christopher T. Russell  and Robert J. Strangeway *University of California, Los Angeles, California 90095-1567, USA*Roy B. Torbert *University of New Hampshire, Durham, New Hampshire 03824, USA*

Thomas E. Moore

*NASA Goddard Space Flight Center, Greenbelt, Maryland 20771, USA*James L. Burch *Southwest Research Institute, San Antonio, Texas 78238-5166, USA*

(Received 2 January 2020; revised manuscript received 3 April 2020; accepted 18 May 2020; published 24 June 2020)

A familiar problem in space and astrophysical plasmas is to understand how dissipation and heating occurs. These effects are often attributed to the cascade of broadband turbulence which transports energy from large scale reservoirs to small scale kinetic degrees of freedom. When collisions are infrequent, local thermodynamic equilibrium is not established. In this case the final stage of energy conversion becomes more complex than in the fluid case, and both pressure-dilatation and pressure strain interactions ($\Pi\text{-D} \equiv -\Pi_{ij}D_{ij}$) become relevant and potentially important. $\Pi\text{-D}$ in plasma turbulence has been studied so far primarily using simulations. The present study provides a statistical analysis of $\Pi\text{-D}$ in the Earth's magnetosheath using the unique measurement capabilities of the Magnetospheric Multiscale (MMS) mission. We find that the statistics of $\Pi\text{-D}$ in this naturally occurring plasma environment exhibit strong resemblance to previously established fully kinetic simulations results. The conversion of energy is concentrated in space and occurs *near* intense current sheets, but not within them. This supports recent suggestions that the chain of energy transfer channels involves regional, rather than pointwise, correlations.

DOI: [10.1103/PhysRevLett.124.255101](https://doi.org/10.1103/PhysRevLett.124.255101)

The study of dissipation processes in space and astrophysical plasmas is of great significance both as a fundamental plasma physics problem and due to its implications

for observed macroscopic effects. In the case of weakly collisional dynamics, typical of these space and astrophysical plasmas [1,2], fluid closures become questionable and

fully kinetic treatment is required [1,3]. For weak collisionality, the usual sign-definite dissipation functions that emerge from Chapman-Enskog ordering are no longer applicable and consequently, the entire subject of dissipation of turbulence and subsequent heating becomes challenging and even elusive. Even if turbulent dissipation is considered a leading candidate for explaining the heating of space plasmas, questions remain, such as the following: What are the rates of transfer of energy through the available kinetic channels? or perhaps, How is the turbulent fluctuation energy transferred into internal degrees of freedom of various plasma species? We examine these questions, adopting a statistical approach, using the unique capabilities of the Magnetospheric Multiscale (MMS) mission [4–6]. We are particularly interested in comparing the observational results with recently reported similar analyses obtained from kinetic plasma simulation [7,8], and this direct approach is enabled by the high-resolution, multispacecraft data that the MMS mission provides.

When equations of energy exchange are computed from the hierarchy of the Vlasov-Maxwell equations, one finds [7,8], for each species, here labeled by α ,

$$\partial_t \mathcal{E}_\alpha^f + \nabla \cdot (\mathcal{E}_\alpha^f \mathbf{u}_\alpha + \mathbf{P}_\alpha \cdot \mathbf{u}_\alpha) = (\mathbf{P}_\alpha \cdot \nabla) \cdot \mathbf{u}_\alpha + n_\alpha q_\alpha \mathbf{E} \cdot \mathbf{u}_\alpha. \quad (1)$$

$$\partial_t \mathcal{E}_\alpha^{\text{th}} + \nabla \cdot (\mathcal{E}_\alpha^{\text{th}} \mathbf{u}_\alpha + \mathbf{h}_\alpha) = -(\mathbf{P}_\alpha \cdot \nabla) \cdot \mathbf{u}_\alpha. \quad (2)$$

$$\partial_t \mathcal{E}^m + \frac{c}{4\pi} \nabla \cdot (\mathbf{E} \times \mathbf{B}) = -\mathbf{E} \cdot \mathbf{j} \quad (3)$$

where q_α is the charge, n_α is the number density, \mathbf{u}_α is the velocity, \mathcal{E}_α^f is the flow energy, \mathbf{P}_α is the pressure tensor, $\mathcal{E}_\alpha^{\text{th}}$ is the trace of pressure tensor designating internal energy, and \mathbf{h}_α is the heat flux for the species α . \mathcal{E}^m is the electromagnetic energy, \mathbf{E} is the electric field, \mathbf{B} is the magnetic field, and \mathbf{j} is the current density. The divergence terms are responsible for transporting energy spatially but they do not convert energy from one form to another. Furthermore, their effects integrate (by Gauss's law) to a surface effect for any finite volume. Therefore they have no net contribution for infinite (or very large) system size or for periodic boundary conditions (relevant for simulations).

The basic physics embodied in Eqs. (1)–(3) is as follows: The term that converts energy between electromagnetic fields and particles is the well known $\mathbf{j} \cdot \mathbf{E}$ term. However it is clear from Eqs. (1) and (2) that $\mathbf{j} \cdot \mathbf{E}$ only converts energy between fields and the bulk flow of each species of particles, but not into the internal energy. The only term that converts energy into internal energy is the pressure strain interaction $\text{PS} = -(\mathbf{P}_\alpha \cdot \nabla) \cdot \mathbf{u}_\alpha$ that converts bulk flow energy into internal energy of each species. This conversion of form of energy into internal energy is what we mean by “dissipation.” This effect has been shown [8,9]

to occur at kinetic scales, hence the terminology “kinetic dissipation.”

The PS interaction can be further decomposed into two parts: $-(\mathbf{P} \cdot \nabla) \cdot \mathbf{u} = -p\delta_{ij}\partial_j u_i - (P_{ij} - p\delta_{ij})\partial_j u_i = -p\theta - \Pi_{ij}D_{ij}$; where $p = \frac{1}{3}P_{ii}$, $\Pi_{ij} = P_{ij} - p\delta_{ij}$, $\theta = \nabla \cdot \mathbf{u}$ and $D_{ij} = \frac{1}{2}(\partial_i u_j + \partial_j u_i) - \frac{1}{3}\theta\delta_{ij}$. Here, δ_{ij} is the Kronecker delta function. The $p\theta$ term is the familiar dilatation term responsible for compressive heating and cooling in fluid models. The term involving the traceless tensor Π becomes the viscous term via the Chapman-Enskog expansion in the collisional limit. In case of collisionless systems, this term does not have a closure but can be explicitly evaluated in simulations and multispacecraft datasets such as MMS. We call this the $-\Pi_{ij}D_{ij}$ term, including the “-” sign, as the “Pi-D” interaction [10,11].

Pi-D acts intermittently in kinetic plasmas near intense intermittent structures such as strong current sheets, reconnection sites [8,9,12,13], and vorticity concentrations [14]. Shearing magnetic islands produce intense current sheets, which in turn produce quadrupole vortex structures nearby [15,16]. Vorticity is the antisymmetric part of the velocity strain tensor and does not contribute to a full contraction with the symmetric tensor Π_{ij} . In plasma turbulence, vorticity concentrations can be produced by velocity shear, as it occurs in hydrodynamics, and also by reconnectionlike activity near current sheets, which is known to produce nearby quadrupolar vortex structures in both 2D [15,16] and 3D [17,18] numerical experiments. In large Reynolds number turbulence these vortices are stretched into sheet-like structures, generating symmetric strain D_{ij} [7,11,16]. The association [16] of vortex structures, co-located concentrations of symmetric strain, and nearby electric current density has been demonstrated in 2D and 3D simulations [8,16,19]. This complex set of dynamical couplings appears to be generic, and provides an explanation for the connection between vorticity and heating [11,16,20]. Notably, recent magnetosheath observations have revealed a new type of coherent structures, namely, electron vortex magnetic holes [21–23], which show correlation of electron vorticity with the increase of electron temperature, making them a possible candidate for electron heating.

To cover a large statistical sample of the turbulent magnetosheath plasma, here we focus on a 40-min MMS burst-mode interval between 06:12:43 and 06:52:23 UTC on 26 December 2017, encompassing several (~ 400) correlation scales. At this time, the interplanetary solar wind had an average magnetic field of 6 nT, flow speed 450 km s⁻¹, and density 6 cm⁻³. The MMS spacecraft, separated by ~ 20 km ($\sim 1/2$ ion-inertial length), were downstream ($\sim 1 R_E$) of the quasiparallel bow shock. See Supplemental Material [24] for the location of MMS with respect to nominal magnetopause [25] and bowshock [26]. The magnetosheath interval has a flow speed of 238 km s⁻¹, a density of 22 cm⁻³, and a proton beta 4.5. The average magnetic field is $B_0 \sim 18$ nT with fluctuations

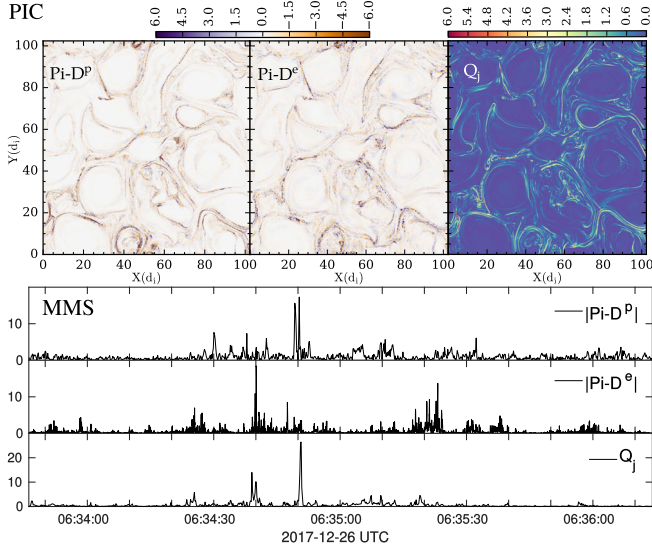


FIG. 1. Normalized Pi-D, $-\Pi_{ij}D_{ij}/(-\Pi_{ij}D_{ij})_{\text{rms}}$, for proton and electron, and normalized current, $Q_j = (1/4)\mathbf{j}^2/\langle\mathbf{j}^2\rangle$ from PIC simulations (top) and a sample of MMS data (bottom).

$\delta b \sim 14$ nT, so that $\delta b/B_0 \sim 0.8$. The interval displays standard features of well-developed turbulence, as previously studied in detail [27].

We compare the MMS observations with the results from a 2.5-dimensional, fully kinetic, particle-in-cell (PIC) simulation [7]. The simulation has 8192^2 grid points, with systems size $L = 102.4d_i$, $\beta_p = \beta_e = 0.1$, $m_p/m_e = 25$, $\delta B/B_0 = 1/5$. We emphasize that no attempt is made to align the simulation parameters with those of the magnetosheath. In fact, one may note that the parameters like plasma beta, magnetic fluctuation amplitude are rather different from the particular interval analyzed here, and magnetosheath conditions [28] in general.

In this Letter, we are interested in the statistics of pressure strain interaction $\text{Pi-D} \equiv -\Pi_{ij}D_{ij}$, which represents the incompressible channel of energy transfer into heat. The computation of D_{ij} requires computation of velocity derivatives. The small separation in tetrahedron formation allows us to employ a straightforward variation of the curlometer technique [29], enabling evaluation of the velocity strain tensor. Several previous studies have found that the curlometer technique is usually accurate for MMS data in the magnetosheath, e.g., Refs. [30–32], although for some particular events, such as near large spatial gradients, the method may not be satisfactory [33]. For this particular interval, however, we find a reasonable agreement between the particle-velocity and curlometer current (see Supplemental Material [24]). The small

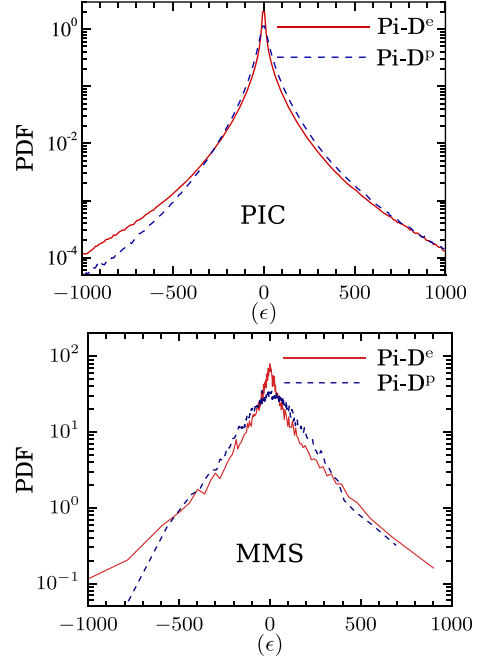


FIG. 2. Probability distribution functions of Pi-D for protons (red solid line) as well as electrons (blue, dashed line) in (top) PIC simulations and (bottom) the magnetosheath from MMS data. The Pi-D values are normalized to the estimate of large-scale decay rate ϵ (see text.) A tendency for protons to have slightly larger Pi-D can be seen. A slight preference for having higher positive tails is clear for both species.

elongation ($E \sim 0.3$) and planarity ($P \sim 0.4$) parameter values of the MMS tetrahedron configuration indicate adequate spatial coverage of the fluctuations [34], so that one expects that the results are reliable. The pressure tensor is averaged over the four MMS spacecraft. The different temporal cadence of the MMS electron and ion measurements might, in principle, affect the comparison of the heating channels. However, we have found that the following results remain qualitatively unchanged, when performed with the electron data resampled to ion cadence (see Supplemental Material [24]).

The proton and electron Pi-D, normalized by their rms fluctuations, are shown in Fig. 1, along with normalized current density. The intermittency of Pi-D is evident in the burstiness of these signals, with enhanced values concentrated in thin, sheetlike structures, occurring near enhanced current density values.

We emphasize that Pi-D is a signed quantity in collisionless plasmas, as energy may be transferred into or out of the collective fluid motion. While pointwise

TABLE I. Turbulent heating measures from estimated evaluations at different scales.

$\epsilon_{\text{von Karman}} (\text{J m}^{-3} \text{s}^{-1})$	$\epsilon_{\text{inertial}} (\text{J m}^{-3} \text{s}^{-1})$	$\langle \text{Pi} - \text{D}^p \rangle (\text{J m}^{-3} \text{s}^{-1})$	$\langle \text{Pi} - \text{D}^e \rangle (\text{J m}^{-3} \text{s}^{-1})$
$(12.8 \pm 0.4) \times 10^{-14}$	$(9.4 \pm 0.3) \times 10^{-14}$	$(5 \pm 2) \times 10^{-13}$	$(4 \pm 1) \times 10^{-13}$

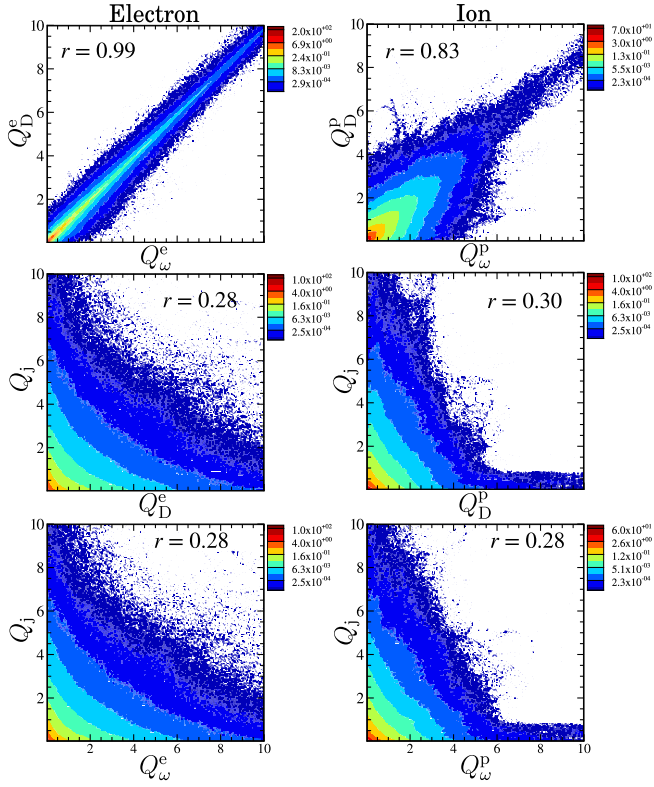


FIG. 3. Joint probability distribution function of the normalized second invariants, $Q_\omega = (1/4)\omega^2/\langle\omega^2\rangle$, $Q_D = (1/4)D_{ij}D_{ij}/\langle D_{ij}D_{ij}\rangle$, and $Q_j = (1/4)\mathbf{j}^2/\langle\mathbf{j}^2\rangle$ for electrons (left column) and protons (right column) from PIC data [8]. Pearson correlation coefficient (r) is shown for each panel.

these quantities are not sign definite, the expectation is that when there is net dissipation and heating, the appropriate sign indicating net transfer into random motions will be favored. In contrast, in the case of viscous dissipation in collisional media, the Pi-D is positive definite by construction. Nevertheless, the computed mean value for Pi-D over the MMS interval is, for protons, $\langle -\Pi_{ij}D_{ij} \rangle = 4.8 \times 10^{-13} \text{ J m}^{-3} \text{ s}^{-1}$, and, for electrons, $4.5 \times 10^{-13} \text{ J m}^{-3} \text{ s}^{-1}$. This indicates a net transfer of energy from turbulence into random internal degrees of freedom during this interval.

To establish a clear connection of the collisionless dissipation measure, Pi-D, with the fluid-scale energy transfer rates, we compare the net (averaged) Pi-D with the MHD measures of decay rate. We evaluate the von Kármán law and third-order law, in a manner similar to that performed in [35]. Table I reports the approximate values of energy-transfer rate, obtained from the three constructs, at different ranges of scale, and the proton and electron Pi-D averages.

There is a reasonable level of agreement among the three measures, indicating an approximate validity of the general scheme of fluid-scale energy cascade, eventually heating the protons and electrons. Variability is likely due to poor statistics, anisotropy of the turbulence, and the possibility of coupling with the compressive channel of

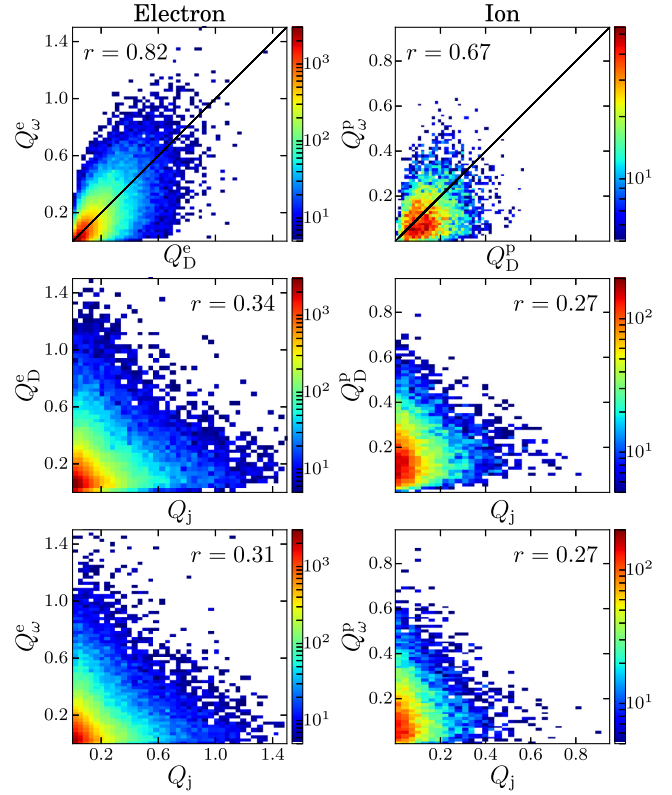


FIG. 4. Same as Fig. 3, but obtained from MMS observations.

energy conversion. A detailed statistical survey with many MMS intervals would help to clarify some of these issues.

The average rate of incompressible heating as well as associated fluctuations may also be seen by examining the probability distribution functions (PDFs) of Pi-D for both species, illustrated in Fig. 2. To make a more direct comparison of the simulation and observation, we normalize the Pi-D values to the global decay rates, ϵ . In simulations, this is evaluated simply by computing the rate of change of total (magnetic + flow) energy, and for MMS data the von Kármán estimate (Table I) is used. The curves are highly non-Gaussian, providing an additional indication of the intermittent distribution of Pi-D. The total kurtosis, defined for variable x as $\kappa = \langle (x - \langle x \rangle)^4 \rangle / \langle (x - \langle x \rangle)^2 \rangle^2$, is 24.6 for the ion Pi-D and 41.6 for the electron Pi-D. The high values of kurtosis reflect the strong intermittency in these variables.

The burstiness of Pi-D, as seen in Fig. 1, suggests correlations with current density, as well as other physical quantities, such as vorticity ($\boldsymbol{\omega} = \nabla \times \mathbf{u}$) and symmetric velocity strain (D_{ij}), which often exhibit similar nonuniform distribution in plasmas. We can examine such possibilities by studying the spatial concentration of Pi-D in comparison with D_{ij} , $\boldsymbol{\omega}$, and \mathbf{j} . We normalize the three second-order invariants as $Q_\omega = (1/4)\omega^2/\langle\omega^2\rangle$, $Q_D = (1/4)D_{ij}D_{ij}/\langle D_{ij}D_{ij}\rangle$, and $Q_j = (1/4)\mathbf{j}^2/\langle\mathbf{j}^2\rangle$. The invariant Q_ω

represents rotation, Q_D corresponds to straining motions, and Q_j is related to magnetic gradients. All of them can interact with one another. To explore the spatial correlation of these processes, we show the joint PDF of the normalized second invariants for each species in Fig. 3 and Fig. 4. To obtain a quantitative assessment, we report the Pearson linear correlation coefficient for each pair of invariants.

From the top two panels in Fig. 3 and Fig. 4, the joint PDFs of Q_ω and Q_D are dominated by a population near the $Q_\omega = Q_D$ line, demonstrating a strong spatial correlation between the two quantities. This strong correlation, found here in plasma turbulence, resembles similar results in hydrodynamic turbulence in regimes in which vorticity is sheetlike rather than tubelike [36,37]. Further, similar to what is observed from the plasma simulations (Fig. 3), the positive correlation in MMS observation is very prominent for electrons, but somewhat weaker in the case of protons (Fig. 4). Although, the better correlation for the case of the electrons in MMS data may be a result of larger statistical sample and better accuracy due to a higher temporal resolution. We note that, if this result were to be established as accurate, it would imply that electron vorticity has a very strong tendency to appear in sheets. The joint PDFs of Q_j versus Q_D , in contrast, are spread broadly, with low correlation coefficients, indicating weak pointwise correlation between these quantities. Similarly, the joint PDFs of Q_j versus Q_ω exhibit weak correlation with a small correlation coefficient both for the PIC and MMS case. Therefore, the vorticity and traceless strain-rate tensor do not correlate pointwise with current density, but are slightly offset in space.

To quantify the spatial correlation between Pi-D and symmetric velocity stress, vorticity, and current density, we compute the conditional averages of Pi-D with these quantities. Figure 5 plots the conditional averages of $-\Pi_{ij}D_{ij}$, separately for protons and electrons. The conditions are based on values of the second tensor invariants Q_D , Q_ω , and Q_j . For example, to compute $\langle -\Pi_{ij}D_{ij}|Q_j \rangle$, one calculates the average of the electron Pi-D including only the values occurring at times when the mean-square total electric current density (Q_j) exceeds a selected threshold. The figure indicates that, for both electrons and protons, elevated levels of $\Pi_{ij}D_{ij}$ are found in regions with enhanced vorticity and in regions of enhanced symmetric stress, consistent with earlier reports [7,8]. In contrast, the averages of Pi-D conditioned on total current density remain fairly constant for protons, and slightly decrease for electrons. The values of Pi-D for protons are even more elevated in regions of large symmetric stress than in regions of large (mean-square) vorticity. The similarity to the analogous results obtained from kinetic simulations in Ref. [38] is once again striking, suggesting that the properties reported here are fundamental to weakly collisional plasmas, and not particular to a specific set of parameters.

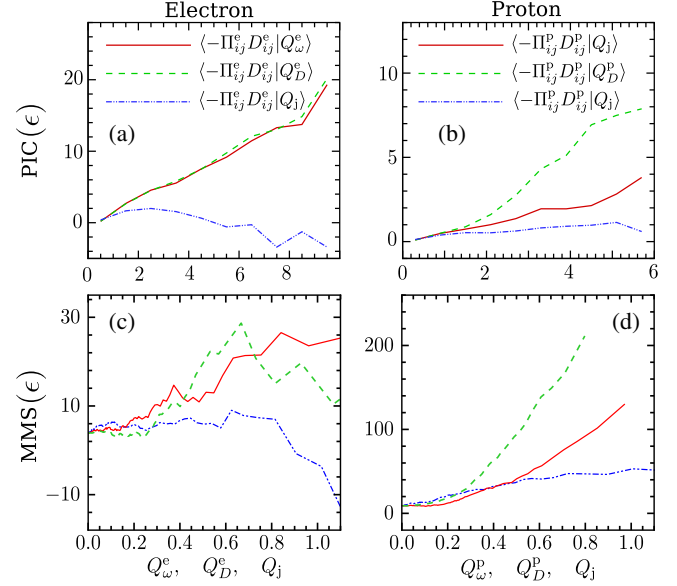


FIG. 5. Conditional averages of the electron (a) and proton (b) Pi-D term from PIC simulation (top); and the same from MMS data [bottom, (c),(d)]. The Pi-D values are normalized to large-scale decay rates ϵ (see text).

Although the results are in qualitative agreement, the range of values of some variables is sometimes quite different in the two systems, especially for the protons in Fig. 5. For example, the ranges of normalized proton Pi-D values in Fig. 5, are different. Such disparity in the two systems is likely attributable to the artificial simulation mass ratio, different scale separations and system sizes, and differences in large-scale driving mechanisms.

In this Letter, we have presented a statistical characterization, of the direct pathways to production of internal energy in collisionless plasma turbulence. In particular we employ MMS observations in the terrestrial magnetosheath to quantify production of internal energy through the pressure-strain interaction, namely, the $-\Pi_{ij}D_{ij}$ term. Previous studies have computed Pi-D in individual events, such as current sheets [39]. The present study is the first one we are aware of that has derived statistical distributions of pressure strain from a large continuous dataset. It is important to recall that the statistics of pressure strain provide a direct quantitative measure of internal energy production without the usual restrictions inherent in selection in advance of a particular wave-mode or mechanism. In this way the present results provide insights into dissipation that are potentially more general than those based on specific mechanisms. Direct comparison between statistics obtained from simulation and from MMS observations shows a remarkable qualitative level of agreement. Note that additional supporting analysis, including an additional MMS interval, is provided as Supplemental Material [24], with a conclusion consistent with those shown here.

The scale-to-scale energy transfer process has been well studied in the energy-containing and inertial range [35,40,41], but the energy conversion processes in the kinetic ranges are not understood. The results presented in this Letter provide a step towards that direction, suggesting correlations and channels of energy conversion that with further study may provide broader insights into these essential plasma physics processes.

The data used in this analysis are Level 2 FIELDS and FPI data products, in cooperation with the instrument teams and in accordance with their guidelines. All MMS data are available at Ref. [42]. The Wind data, shifted to the Earth's bow-shock nose, can be found at Ref. [43].

This research was supported in part by the MMS Theory and Modeling team grant under NASA Grant No. NNX14AC39 and No. 80NSSC19K0565, and by NASA Heliophysics SRT Grant No. NNX17AB79G. We are grateful to the MMS instrument teams for cooperation and collaboration in preparing the data. The authors thank the Wind team for the magnetic field and proton moment dataset.

*Corresponding author.

riddhib@udel.edu

†Present address: School of Chemical and Physical Sciences, Victoria University of Wellington, Kelburn, Wellington 6012, New Zealand.

- [1] E. Quataert, *Astron. Nachr.* **324**, 435 (2003).
- [2] E. Marsch, *Living Rev. Solar Phys.* **3**, 1 (2006).
- [3] C. Wang and J. Richardson, *J. Geophys. Res.* **106**, 29401 (2001).
- [4] J. L. Burch, T. E. Moore, R. B. Torbert, and B. L. Giles, *Space Sci. Rev.* **199**, 5 (2016).
- [5] C. Pollock *et al.*, *Space Sci. Rev.* **199**, 331 (2016).
- [6] C. T. Russell *et al.*, *Space Sci. Rev.* **199**, 189 (2016).
- [7] Y. Yang, W. H. Matthaeus, T. N. Parashar, P. Wu, M. Wan, Y. Shi, S. Chen, V. Roytershteyn, and W. Daughton, *Phys. Rev. E* **95**, 061201(R) (2017).
- [8] Y. Yang, W. H. Matthaeus, T. N. Parashar, C. C. Haggerty, V. Roytershteyn, W. Daughton, M. Wan, Y. Shi, and S. Chen, *Phys. Plasmas* **24**, 072306 (2017).
- [9] Y. Yang, M. Wan, W. H. Matthaeus, L. Sorriso-Valvo, T. N. Parashar, Q. Lu, Y. Shi, and S. Chen, *Mon. Not. R. Astron. Soc.* **482**, 4933 (2019).
- [10] D. Del Sarto, F. Pegoraro, and F. Califano, *Phys. Rev. E* **93**, 053203 (2016).
- [11] D. Del Sarto and F. Pegoraro, *Mon. Not. R. Astron. Soc.* **475**, 181 (2018).
- [12] M. Sitnov, V. Merkin, V. Roytershteyn, and M. Swisdak, *Geophys. Res. Lett.* **45**, 4639 (2018).
- [13] O. Pezzi, Y. Yang, F. Valentini, S. Servidio, A. Chasapis, W. Matthaeus, and P. Veltri, *Phys. Plasmas* **26**, 072301 (2019).
- [14] D. Del Sarto, F. Pegoraro, and F. Califano, *Phys. Rev. E* **93**, 053203 (2016).
- [15] W. H. Matthaeus, *Geophys. Res. Lett.* **9**, 660 (1982).
- [16] T. N. Parashar and W. H. Matthaeus, *Astrophys. J.* **832**, 57 (2016).
- [17] V. Zhdankin, D. A. Uzdensky, J. C. Perez, and S. Boldyrev, *Astrophys. J.* **771**, 124 (2013).
- [18] M. Wan, A. F. Rappazzo, W. H. Matthaeus, S. Servidio, and S. Oughton, *Astrophys. J.* **797**, 63 (2014).
- [19] A. Chasapis, Y. Yang, W. H. Matthaeus, T. N. Parashar, C. C. Haggerty, J. L. Burch, T. E. Moore, C. J. Pollock, J. Dorelli, D. J. Gershman, R. B. Torbert, and C. T. Russell, *Astrophys. J.* **862**, 32 (2018).
- [20] L. Franci, P. Hellinger, L. Matteini, A. Verdini, and S. Landi, *AIP Conf. Proc.* **1720**, 040003 (2016).
- [21] S. Y. Huang *et al.*, *Astrophys. J. Lett.* **836**, L27 (2017).
- [22] S. Y. Huang, J. W. Du, F. Sahraoui, Z. G. Yuan, J. S. He, J. S. Zhao, O. Le Contel, H. Breuillard, D. D. Wang, X. D. Yu, X. H. Deng, H. S. Fu, M. Zhou, C. J. Pollock, R. B. Torbert, C. T. Russell, and J. L. Burch, *J. Geophys. Res.* **122**, 8577 (2017).
- [23] S. Y. Huang, F. Sahraoui, Z. G. Yuan, O. Le Contel, H. Breuillard, J. S. He, J. S. Zhao, H. S. Fu, M. Zhou, X. H. Deng, X. Y. Wang, J. W. Du, X. D. Yu, D. D. Wang, C. J. Pollock, R. B. Torbert, and J. L. Burch, *Astrophys. J.* **861**, 29 (2018).
- [24] See Supplemental Material at <http://link.aps.org/supplemental/10.1103/PhysRevLett.124.255101> for MMS location, discussion of quality of curlometer technique, and additional supporting analysis, including more MMS interval.
- [25] J.-H. Shue, P. Song, C. T. Russell, J. T. Steinberg, J. K. Chao, G. Zastenker, O. L. Vaisberg, S. Kokubun, H. J. Singer, T. R. Detman, and H. Kawano, *J. Geophys. Res.* **103**, 17691 (1998).
- [26] M. H. Farris and C. T. Russell, *J. Geophys. Res.* **99**, 17681 (1994).
- [27] T. N. Parashar, A. Chasapis, R. Bandyopadhyay, R. Chhiber, W. H. Matthaeus, B. Maruca, M. A. Shay, J. L. Burch, T. E. Moore, B. L. Giles, D. J. Gershman, C. J. Pollock, R. B. Torbert, C. T. Russell, R. J. Strangeway, and V. Roytershteyn, *Phys. Rev. Lett.* **121**, 265101 (2018).
- [28] S. Y. Huang, L. Z. Hadid, F. Sahraoui, Z. G. Yuan, and X. H. Deng, *Astrophys. J. Lett.* **836**, L10 (2017).
- [29] M. Dunlop, D. Southwood, K.-H. Glassmeier, and F. Neubauer, *Adv. Space Res.* **8**, 273 (1988).
- [30] D. B. Graham, Y. V. Khotyaintsev, C. Norgren, A. Vaivads, M. André, P.-A. Lindqvist, G. T. Marklund, R. E. Ergun, W. R. Paterson, D. J. Gershman, B. L. Giles, C. J. Pollock, J. C. Dorelli, L. A. Avanov, B. Lavraud, Y. Saito, W. Magnes, C. T. Russell, R. J. Strangeway, R. B. Torbert, and J. L. Burch, *Geophys. Res. Lett.* **43**, 4691 (2016).
- [31] D. J. Gershman, A. F. Vinas, J. C. Dorelli, M. L. Goldstein, J. Shuster, L. A. Avanov, S. A. Boardsen, J. E. Stawarz, S. J. Schwartz, C. Schiff, B. Lavraud, Y. Saito, W. R. Paterson, B. L. Giles, C. J. Pollock, R. J. Strangeway, C. T. Russell, R. B. Torbert, T. E. Moore, and J. L. Burch, *Phys. Plasmas* **25**, 022303 (2018).
- [32] J. E. Stawarz, J. P. Eastwood, T. D. Phan, I. L. Gingell, M. A. Shay, J. L. Burch, R. E. Ergun, B. L. Giles, D. J. Gershman, O. Le Contel, P. A. Lindqvist, C. T. Russell, R. J. Strangeway, R. B. Torbert, M. R. Argall, D. Fischer, W. Magnes, and L. Franci, *Astrophys. J. Lett.* **877**, L37 (2019).

- [33] M. Akhavan-Tafti, J. A. Slavin, G. Le, J. P. Eastwood, R. J. Strangeway, C. T. Russell, R. Nakamura, W. Baumjohann, R. B. Torbert, B. L. Giles, D. J. Gershman, and J. L. Burch, *J. Geophys. Res.* **123**, 1224 (2018).
- [34] P. Robert, M. W. Dunlop, A. Roux, and G. Chanteur, *Analysis Methods for Multi-Spacecraft Data*, edited by G. Paschmann and P. Daly, ISSI Scientific Reports Series, ESA/ISSI Vol. 1 (1998), pp. 395–418, <https://ui.adsabs.harvard.edu/abs/1998ISSIR...1..395R/abstract>.
- [35] R. Bandyopadhyay, A. Chasapis, R. Chhiber, T. N. Parashar, W. H. Matthaeus, M. A. Shay, B. A. Maruca, J. L. Burch, T. E. Moore, C. J. Pollock, B. L. Giles, W. R. Paterson, J. Dorelli, D. J. Gershman, R. B. Torbert, C. T. Russell, and R. J. Strangeway, *Astrophys. J.* **866**, 106 (2018).
- [36] J. Jiménez, A. A. Wray, P. G. Saffman, and R. S. Rogallo, *J. Fluid Mech.* **255**, 65 (1993).
- [37] H. M. Blackburn, N. N. Mansour, and B. J. Cantwell, *J. Fluid Mech.* **310**, 269 (1996).
- [38] Y. Yang, W. H. Matthaeus, Y. Shi, M. Wan, and S. Chen, *Phys. Fluids* **29**, 035105 (2017).
- [39] A. Chasapis, W. H. Matthaeus, T. N. Parashar, M. Wan, C. C. Haggerty, C. J. Pollock, B. L. Giles, W. R. Paterson, J. Dorelli, D. J. Gershman, R. B. Torbert, C. T. Russell, P. A. Lindqvist, Y. Khotyaintsev, T. E. Moore, R. E. Ergun, and J. L. Burch, *Astrophys. J. Lett.* **856**, L19 (2018).
- [40] M. K. Verma, *Phys. Rep.* **401**, 229 (2004).
- [41] J. T. Coburn, M. A. Forman, C. W. Smith, B. J. Vasquez, and J. E. Stawarz, *Phil. Trans. R. Soc. A* **373**, 20140150 (2015).
- [42] <https://lasp.colorado.edu/mms/sdc/>.
- [43] <https://omniweb.gsfc.nasa.gov/>.